

PAPER • OPEN ACCESS

## Adaptive ultrasound reflectometry for lubrication film thickness measurements

To cite this article: R L Kaeseler and P Johansen 2020 *Meas. Sci. Technol.* **31** 025108

View the [article online](#) for updates and enhancements.

### You may also like

- [Density fluctuation correlation measurements in ASDEX Upgrade using poloidal and radial correlation reflectometry](#)  
D Prisiazhniuk, G D Conway, A Krämer-Flecken et al.
- [H-mode filament studies with reflectometry in ASDEX upgrade](#)  
J Vicente, G D Conway, M E Manso et al.
- [2D full-wave simulations of conventional reflectometry using 3D gyro-fluid plasma turbulence](#)  
J Vicente, T Ribeiro, F Da Silva et al.

# Adaptive ultrasound reflectometry for lubrication film thickness measurements

R L Kaeseler and P Johansen 

Department of Energy Technology, Pontoppidanstraede 111, 9220 Aalborg East, Denmark

E-mail: [pjo@et.aau.dk](mailto:pjo@et.aau.dk)

Received 25 September 2018, revised 14 June 2019

Accepted for publication 26 July 2019

Published 18 November 2019



## Abstract

Adaptive ultrasound reflectometry methods for lubrication film thickness measurements is of great use for condition monitoring and prognostics of systems which have high repair costs and are remotely located, such as off-shore systems, as they recursively calibrate the incident ultrasound wave. Typical manual calibration requires a constant incident wave over the life-cycle of the system, or until new manual calibration can be conducted. Auto-calibration accounts for the changes in the incident ultrasound wave caused by changing environmental conditions, occurring over longer periods of time. The vision of adaptive ultrasound reflectometry methods is therefore increased robustness of lubrication film thickness measurements in a range of applications. In this article an adaptive scheme is proposed. The scheme is based on a thin-layer time-of-flight method for thickness determination, and an extended Kalman filter for estimation of the incident wave spectrum. The adaptive scheme is experimentally tested, and the feasibility of the algorithm is established, but serious issues regarding the robustness and reliability of the method are revealed by a disturbance analysis. However, the experiments and a theoretical layer phase-lag sensitivity analysis reveal that the estimation of the incident wave phase is of high importance for layer thicknesses above 20  $\mu\text{m}$ , and for very thin layers below 1  $\mu\text{m}$  the estimation of the magnitude dominates the measurement accuracy. This entails that the research in adaptive schemes should be directed towards phase- or magnitude-tracking performance, depending on the working range of the layer thickness, such that sufficient robustness and reliability of the algorithms can be assured.

Keywords: ultrasound, tribology, lubrication, film thickness, thin layer, reflectometry


(Some figures may appear in colour only in the online journal)

## 1. Introduction

Most mechanical systems use lubrication to increase efficiency and decrease wear damage caused by tribological contact between moving parts. A main research challenge in tribology today is to advance design procedures beyond costly empirical trial-and-error methods by theoretical studies [1–3]. A significant challenge in this regard is the experimental techniques at the engineer's disposal for validation of virtual prototypes. Experimental measurement methods, which are non-invasive with respect to the tribodynamics, for the determination of

lubricating film thickness are of great interest for this purpose. In addition, such methods are useful in condition monitoring, diagnosis, prognostics and predictive maintenance. It is especially useful at locations with high repair costs, such as off-shore systems, where it is reasonable to monitor tribological performance. In this regard it would be of great potential to use non-invasive tribological measurement methods, with capabilities to provide sufficiently accurate measurements, while being robust in varying environmental conditions.

Ultrasound-based thin-layer thickness measurements is a very appealing non-invasive method for determination of lubrication film thicknesses. It has been proven to work in a range of applications, such as journal bearings, liner-piston skirts and internal combustion engine piston rings [4–6]. For estimation of ultrasound time of flight in a thin layer the

 Original content from this work may be used under the terms of the [Creative Commons Attribution 3.0 licence](https://creativecommons.org/licenses/by/3.0/). Any further distribution of this work must maintain attribution to the author(s) and the title of the work, journal citation and DOI.

challenge is to extract the thickness information from the reflections that are overlapping in the time domain. Currently, there are two dominant approaches for detection, either by interpretation via a continuum model or by a lumped parameter approach using a spring interface model.

Pialucha and Cawley [7] consider the continuum model of a three-layered system response. With this model, they analyze the resonating frequency to estimate the time of flight and thereby the thickness. For particular matching ranges of the transducer bandwidth and the film thickness a resonance phenomenon is identifiable in the frequency spectrum of the reflected wave, which allows for estimation of the film thickness. However, a large range of applications does not render this method useful.

Zhang *et al* [8] and Dwyer-Joyce *et al* [9] discussed a simplified spring model, which approximates the fluid layer as a spring. They used this to estimate the thickness of very thin layers. The spring model is only accurate at a small range of thickness, where Zhang *et al* gives the rule of thumb that the method can be used for thickness measurements  $0.1 \leq |R_s| \leq 0.95$ , with  $R_s$  being the spring model reflection coefficient. Dwyer-Joyce *et al* performs a model-bias analysis to investigate the estimation range of the spring model, and indicate that this rule of thumb is a best-case scenario.

Praher and Steinbichler [10] propose a time-domain solution strategy, which determines the time of flight by determining the maximum cross-correlation between the waves. Kaeseler *et al* [11] presents a layer phase-lag method, which uses the phase of the layer spectrum to estimate the thickness. They further discuss the advantages and disadvantages of the spring method, the resonance, the cross-correlation method and lastly the layer phase-lag method. In conclusion, the resonance method is preferred if a resonating frequency exist in the reflected wave spectrum, and its resonating period is known. The cross-correlation method is otherwise preferred if the thickness is above the first resonating frequency, while the layer phase-lag method is preferred if the thickness is below it. The spring method is thus deemed obsolete.

These thickness estimation methods use the transmitted and received ultrasound wave to determine the film thickness, where knowledge of the transmitted wave is required, and thereby necessitates calibration. The most general method for calibration is manually conducted upon installation of the system. This calibration requires the oil layer to be replaced by air, which is the case when disassembling the tribological joint. The reflection coefficient between a solid member of the tribological joint and air is close to unity, whereby the transmitted wave is measured directly by the reflection. The use of manual calibration entails a problematic aspect. The disassembling procedure can be quite problematic in some systems, and for estimation of the reflection coefficient spectrum in such systems the transmitted wave is assumed to be constant over the entire test of the component. This cause a lack of robustness to the effect of changing variables, such as temperature and other environmental disturbances, which can cause change in the transmitted wave.

Reddyhoff *et al* [12] proposes auto-calibration, rather than the traditional manual calibration performed at installation. The advantage of such an algorithm is that small changes in the transmitted wave, occurring over a longer period of time, is adjusted recursively. The algorithm is based on the simple spring model and considers only the case wherein the two solid bodies are of the same material.

Kaeseler and Johansen [13] continued the work of Reddyhoff *et al* by deriving a new regression model from the continuum model, rather than the less exact spring model. The model furthermore includes the case of material difference in the bounding solids, which results in a non-linear regression model. This non-linear equation was however linearized, yielding a similar equation to that presented by Reddyhoff *et al* [12].

In this article an adaptive ultrasound reflectometry algorithm is presented. This algorithm is based on the layer phase-lag method for thickness determination and an extended Kalman filter (EKF) for incident wave estimation. The fundamentals of the approach are firstly introduced, followed by the introduction of the experimental test setup. A series of test results are subsequently presented, and the influence of relative phase and magnitude error is revealed by a sensitivity analysis. Finally, the results of a disturbance test is shown, and the challenges of adaptive ultrasound reflectometry are discussed.

## 2. Time-of-flight estimation in thin layers

When an ultrasound wave hits a boundary between two materials, some energy is reflected back from the boundary in the form of a reflected ultrasound wave, while the remaining energy is transmitted to the second medium. In figure 1 a layered medium model is illustrated. Assuming only longitudinal waves, an ultrasound wave can be described as transmitting waves  $T_i$  going in the positive direction of  $x$ , and reflective waves  $R_i$  going in the negative direction. The tribological system can thus be modeled as a series of pulses being reflected from boundary to boundary as seen in figure 1. Each boundary has a reflection constant, which can be calculated from the acoustic impedances of the mediums.

$$R_1 = \frac{z_a - z_b}{z_a + z_b} \quad R_2 = \frac{z_b - z_c}{z_b + z_c} \quad (1)$$

where  $z_a$ ,  $z_b$  and  $z_c$  is the acoustic impedances.

The problem of measuring the layer thickness can actually be reduced to the problem of finding the time of flight for waves traveling through the thin layer. Considering the transmission  $T_{b0}(t)$  into medium **b** of the incident wave  $T_a(t)$ , continuity require that

$$T_{b0}(t)|_{x=0} = T_a(t)|_{x=0} + R_{a1}(t)|_{x=0} \quad (2)$$

which can be rewritten as

$$T_{b0}(t)|_{x=0} = (1 + R_1)T_a(t)|_{x=0}. \quad (3)$$

Note that the evaluation of waves at  $|_{x=0}$  is consistent in this article, and the explicit notation of spatial evaluation is omitted in the following.

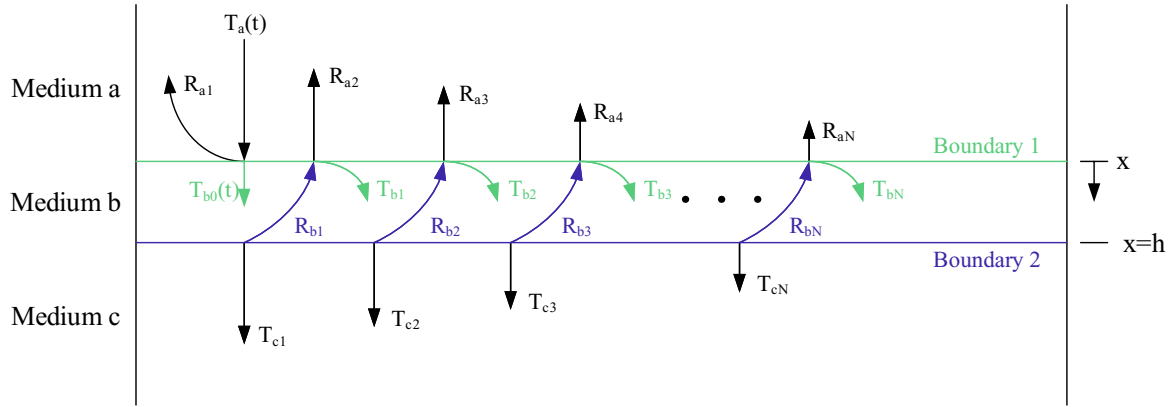


**Figure 1.** The layered system model of the transmitting and reflective waves acting in the oil film and on the medium boundaries.

The transmitted and reflected waves inside the thin layer are expressed as a superposition of multiple reflections from the bounding solids.

$$T_b(t) = \sum_{n=1}^N T_{bn} \quad R_b(t) = \sum_{n=1}^N R_{bn}. \quad (4)$$

The terms in these sums are essentially the transmission of the incident wave  $T_{b0}(t)$ , which is time-shifted and multiplied by the reflection constants  $R_1$  and  $R_2$ .

Evaluating the waves traveling from boundary 2 to boundary 1 in medium **b** yields

$$R_b(t) = R_2 T_{b0}(t - \tau) - R_1 R_2^2 T_{b0}(t - 2\tau) + \dots + (-R_1)^{N-1} R_2^N T_{b0}(t - N\tau) \quad (5)$$

where  $\tau$  is the time of flight from boundary 1 to boundary 2 and back. As the length between boundaries is defined as the layer thickness  $h$  the time of flight  $\tau$  can be calculated using the speed of sound  $c_b$  through medium **b**, such that

$$\tau = \frac{2h}{c_b}. \quad (6)$$

Exploiting the continuity condition in equation (16) the superposition in equation (5) can be expressed in terms of  $T_a(t)$ , such that

$$R_b(t) = (1 + R_1) \sum_{n=1}^N R_2^n (-R_1)^{n-1} T_a(t - n\tau) \quad (7)$$

where  $N$  depends on the duration of the incident wave  $T_a(t)$ .

Using a similar approach for the waves traveling from boundary 1 to boundary 2 then yields

$$T_b(t) = (1 + R_1) T_a(t) + (1 + R_1) \sum_{n=1}^N R_2^n (-R_1)^n T_a(t - n\tau). \quad (8)$$

Equation (7) is advantageously rewritten as

$$R_b(t) = -\frac{(1 + R_1)}{R_1} \sum_{n=1}^N R_2^n (-R_1)^n T_a(t - n\tau) \quad (9)$$

whereby it is directly clear that the last term in equation (8) can be substituted by  $-R_1 R_b(t)$ . Combining equations (7) and (8) leads to a relation between the incident wave and the layer waves, which is expressed as

$$T_b(t) = (1 + R_1) T_a(t) - R_1 R_b(t). \quad (10)$$

Using the continuity condition at boundary 1 given as

$$T_a(t) + R_a(t) = T_b(t) + R_b(t) \quad (11)$$

then yields a linear mapping between waves transmitted  $T_a(t)$  and received  $R_a(t)$ , by the transducer, and the layer waves  $T_b(t)$  and  $R_b(t)$ .

$$\begin{bmatrix} T_b(t) \\ R_b(t) \end{bmatrix} = \frac{1}{1 - R_1} \begin{bmatrix} 1 & -R_1 \\ -R_1 & 1 \end{bmatrix} \begin{bmatrix} T_a(t) \\ R_a(t) \end{bmatrix}. \quad (12)$$

This relation provides the foundation for using time-of-flight methods in thin-layer thickness measurements, because the time lag between  $T_b(t)$  and  $R_b(t)$  is the time of flight  $\tau$ , which is expressed by the speed of the sound  $c_b$  in medium **b** and twice the thickness  $2h$  of medium **b**, such that

$$\tau = \frac{2h}{c_b}. \quad (13)$$

Consequently, the thin-layer thickness estimation problem is reduced to a classical delay estimation problem.

### 3. Layer phase-lag method

The adaptive scheme presented in this article is based on the layer phase-lag method, which essentially is delay estimation using the Fourier transform. This is performed by calculating the layer spectrum  $J(\omega)$ , given as

$$J(\omega) = \frac{\mathcal{F}\{R_b(t)\}}{\mathcal{F}\{T_b(t)\}} = \frac{R(\omega) - R_1}{1 - R_1 R(\omega)} \quad (14)$$

where the reflection coefficient spectrum  $R(\omega)$  is expressed as

$$R(\omega) = \frac{\mathcal{F}\{R_a(t)\}}{\mathcal{F}\{T_a(t)\}}. \quad (15)$$

The layer spectrum  $J(\omega)$  is the transfer function between the layer wave transmitted from boundary 1 to 2 and the layer

waves reflected back from boundary 2 to 1, and this transfer function is given as

$$J(\omega) = R_2 e^{-i\omega\tau}. \quad (16)$$

Consequently, the layer phase-lag method is as follows:

- measure the reflection to the transducer  $R_a(t)$ ;
- calculate the reflection coefficient  $R(\omega)$  (equation (15));
- calculate the layer spectrum  $J(\omega)$  (equation (14));
- calculate the layer spectrum phase  $\omega\tau$ ;
- determine the layer thickness  $h = \frac{2\tau}{c_b}$ .

In total, the layer spectrum phase is used to determine the time of flight, and the layer thickness is subsequently determined. However, it should be noted that the Fourier transform of the incident wave  $\mathcal{F}\{T_a(t)\}$  is assumed to be known. This information is estimated by the adaptive scheme presented in the following.

#### 4. Regression model

In this section the regression model, which provides the basis for estimation of the incident wave  $T_a(t)$ , is presented. This regression model is used in the extended Kalman filter (EKF) to develop an adaptive algorithm for ultrasound reflectometry measurement of the thin-layer thickness.

By definition the magnitude of the layer spectrum  $J(\omega)$  is equal to the reflection constant at boundary 2. Consequently, equation (14) can be rewritten as

$$R_2^2 |1 - R(\omega)R_1|^2 = |R(\omega) - R_1|^2. \quad (17)$$

The reflection coefficient spectrum can advantageously be expressed, in terms of an amplitude  $A(\omega)$ , and phase  $\theta(\omega)$ , such that

$$R(\omega) = A(\omega) (\cos(\theta(\omega)) + i \sin(\theta(\omega))). \quad (18)$$

Using this formulation of the reflection coefficient spectrum in equation (17) yields

$$A^2 K_a + K_b = 2AK_c \cos(\theta) \quad (19)$$

where the constants  $K_a$ ,  $K_b$  and  $K_c$  are given as

$$K_a = 1 - R_1^2 R_2^2 \quad (20)$$

$$K_b = R_1^2 - R_2^2 \quad (21)$$

$$K_c = R_1 (1 - R_2^2). \quad (22)$$

Evaluation of both the incident wave  $T_a$  and received wave  $R_a$  in the frequency domain at frequency  $\omega_i$  is for the purpose of adaptive filtering development reformulated in the real numbers  $\mathcal{R}^2$ , such that

$$\mathbf{y} = \begin{bmatrix} \text{Re}(\mathcal{F}\{R_a(t)\}) \\ \text{Im}(\mathcal{F}\{R_a(t)\}) \end{bmatrix} \Big|_{\omega=\omega_i} \quad (23)$$

$$\mathbf{u} = \begin{bmatrix} \text{Re}(\mathcal{F}\{T_a(t)\}) \\ \text{Im}(\mathcal{F}\{T_a(t)\}) \end{bmatrix} \Big|_{\omega=\omega_i}. \quad (24)$$

The magnitude of the reflection coefficient spectrum, evaluated at a given frequency, is thereby given as

$$A(\omega_i) = |R(\omega_i)| = \frac{|\mathbf{y}|}{|\mathbf{u}|} \Big|_{\omega=\omega_i}. \quad (25)$$

The cosine of the phase shift can be expressed as

$$\left[ \cos(\theta) = \frac{\mathbf{y}^T \mathbf{u}}{|\mathbf{u}| |\mathbf{y}|} \right]_{\omega=\omega_i}. \quad (26)$$

Finally, substitution of equations (26) and (25) into equation (19) leads to

$$[K_a |\mathbf{y}|^2 + K_b |\mathbf{u}|^2 - 2K_c \mathbf{y}^T \mathbf{u}]_{\omega=\omega_i} = 0 \quad (27)$$

which is a non-linear regression model, where the knowledge of the constants  $K_a$ ,  $K_b$  and  $K_c$ , together with measurements of the reflected wave  $\mathbf{y}$ , can be used to estimate the incident wave  $\mathbf{u}$ .

#### 5. EKF based incident wave estimation

To apply the regression model for incident wave estimation an extended Kalman filter (EKF) is used. The non-linear regression model can be rewritten as

$$|\mathbf{y}(t)|^2 = \left( \frac{2K_c}{K_a} \mathbf{y}(t)^T - \frac{K_b}{K_a} \mathbf{u}(t)^T \right) \mathbf{u}(t). \quad (28)$$

This formulation can be applied to a simple form of an EKF algorithm given in equations (29)–(32).

$$\mathbf{v}(t) = \mathbf{v}(t-1)$$

$$+ \mathbf{K}(t) \left( |\mathbf{y}|^2 - \left( \frac{2K_c}{K_a} \mathbf{y}^T - \frac{K_b}{K_a} \mathbf{v}(t-1)^T \right) \mathbf{v}(t-1) \right) \quad (29)$$

$$\mathbf{K}(t) = \frac{\mathbf{P}(t-1) \mathbf{C}(t)^T}{\mathbf{C}(t) \mathbf{P}(t-1) \mathbf{C}(t)^T + 1} \quad (30)$$

$$\mathbf{P}(t) = (\mathbf{I} - \mathbf{K}(t) \mathbf{C}(t)) \mathbf{P}(t-1) \quad (31)$$

where

$$\mathbf{C}(t) = \frac{2K_c}{K_a} \mathbf{y}(t)^T - \frac{2K_b}{K_a} \mathbf{v}(t-1)^T. \quad (32)$$

The incident wave is then determined as

$$\mathcal{F}\{T_a(t)\} = \begin{bmatrix} 1 & i \end{bmatrix} \mathbf{v}(t). \quad (33)$$

The estimated incident wave is used in the layer phase-lag method to estimate the layer thickness, whereby an algorithm which omits the need for manual calibration procedure for incident wave determination is obtained.

#### 6. Experimental testing

To test the functionality of the adaptive scheme an experimental test is conducted. Figure 2 shows the test setup. It consists of a transducer/receiver glued to a steel transducer fixture. This fixture is adjustable and constitutes medium **a**

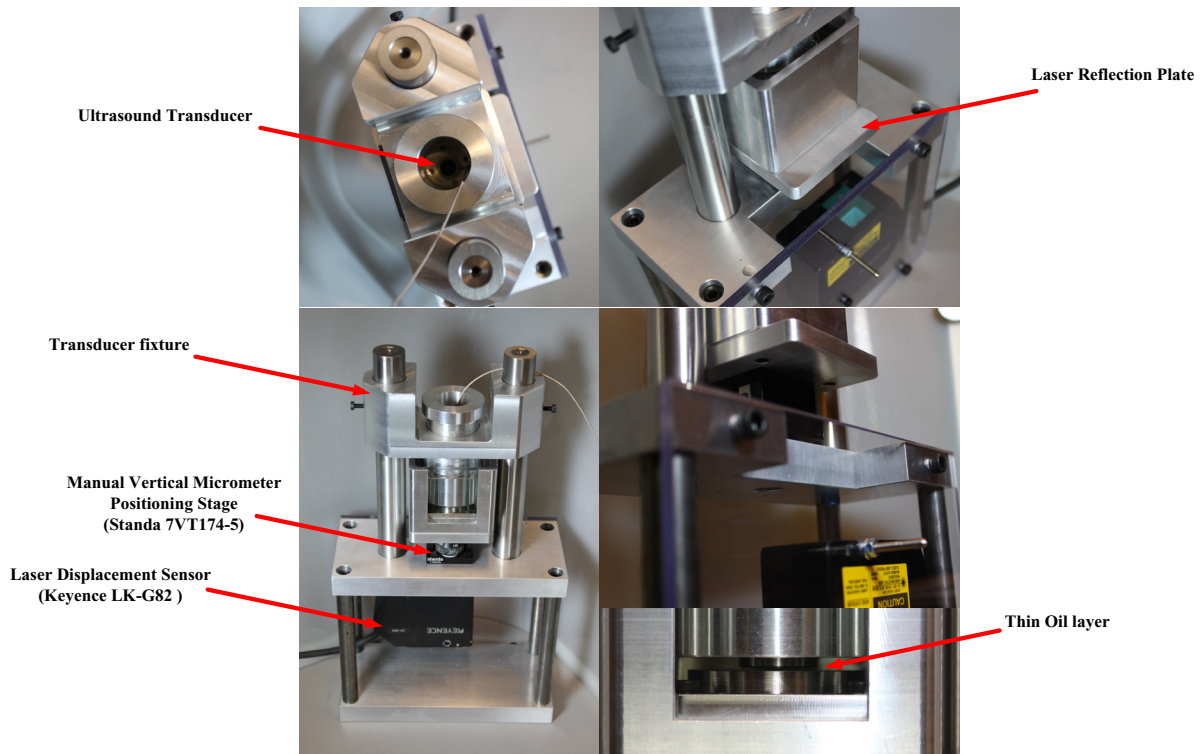


**Figure 2.** Laboratory test setup for ultrasound reflectometry testing with manual micrometer thin-layer thickness adjustment and laser displacement sensor.

in figure 1. The fixture is lowered into a tub filled with ISO VG 46 oil, and in the bottom of the tub a steel back piece constitutes medium  $c$  in figure 1. The tub is placed upon a manual vertical micrometer positioning stage, whereby the thin-layer thickness is adjustable. A laser displacement sensor is placed below the tub to provide reference measurements of the variations in the thin-layer thickness. Note that the laser is not used for absolute position measurements, but for thickness dynamics.

Before the experiments are conducted a manual calibration is performed to obtain the incident wave reference. This is done by raising the transducer fixture out of the tub and carefully removing oil and cleaning the steel boundary, which is equivalent to boundary 1 in figure 1. As the acoustic impedance of air is near zero, and indeed a lot smaller than the acoustic impedance of steel, the steel/air boundary entails a near complete reflection of the incident wave. The received wave is thus approximately the incident wave.

In figures 3–5 three different dynamic test cases are presented. The adaptive algorithm is initiated at  $\mathbf{v}(0) = 0$ . From each test case the lubrication thickness is presented from the manual calibrated ultrasound measurements using the layer phase-lag method, the adaptive ultrasound reflectometry method based on extended Kalman filtering and the laser displacement sensor. Note that the laser displacement results are offset to fit the manual calibrated results, because the laser only measures the variations in the thin-layer thickness.

From the results it is immediately clear that the layer phase-lag method is applicable to measurement of thin film dynamics in the entire range of thicknesses in the test, which spans 20  $\mu\text{m}$  to 80  $\mu\text{m}$ . In figure 3 the lowest layer thickness

is obtained. The test setup entails a lower bound of approximately 20  $\mu\text{m}$ , because the forces needed to squeeze the film further cause elastic deflections that can be detected by a deviation between the variations measured by the laser sensor and the manually calibrated ultrasound reflectometry technique.

All tests reveal that the residual, which is given as

$$\mathbf{Res} = |\mathbf{y}(t)|^2 - \left( \frac{2K_c}{K_a} \mathbf{y}(t)^T + \frac{K_b}{K_a} \mathbf{u}(t)^T \right) \mathbf{u}(t) \quad (34)$$

is converging towards zero for the adaptive scheme as expected. The residual essentially measures how well the incident wave and reflection measurement fits the regression model, and the residual for the manual calibration shows a consistent offset, which may be explained by possible inaccuracy of the fundamental model assumptions, such as the longitudinal wave assumption, or a lack of accuracy in the used material parameters.

The deviations shown in the results are the percentage deviation between the manually calibrated measurements and the adaptive reflectometry measurements. The deviation is observed to vary significantly with time in all test cases. In figure 3 there is a significant deviation throughout the entire test, whereas in figure 5 the deviation is nearly eliminated for a period of time. However, the deviation increases when the dynamics of the thickness is changing.

The relative magnitude and phase error is also shown in the test results. These are calculated as the difference in magnitude and phase between the manually calibrated and adaptive estimated incident wave spectra, which is normalized with respect to the manually calibrated spectrum. An interesting aspect which is revealed by these tests is that the relative error

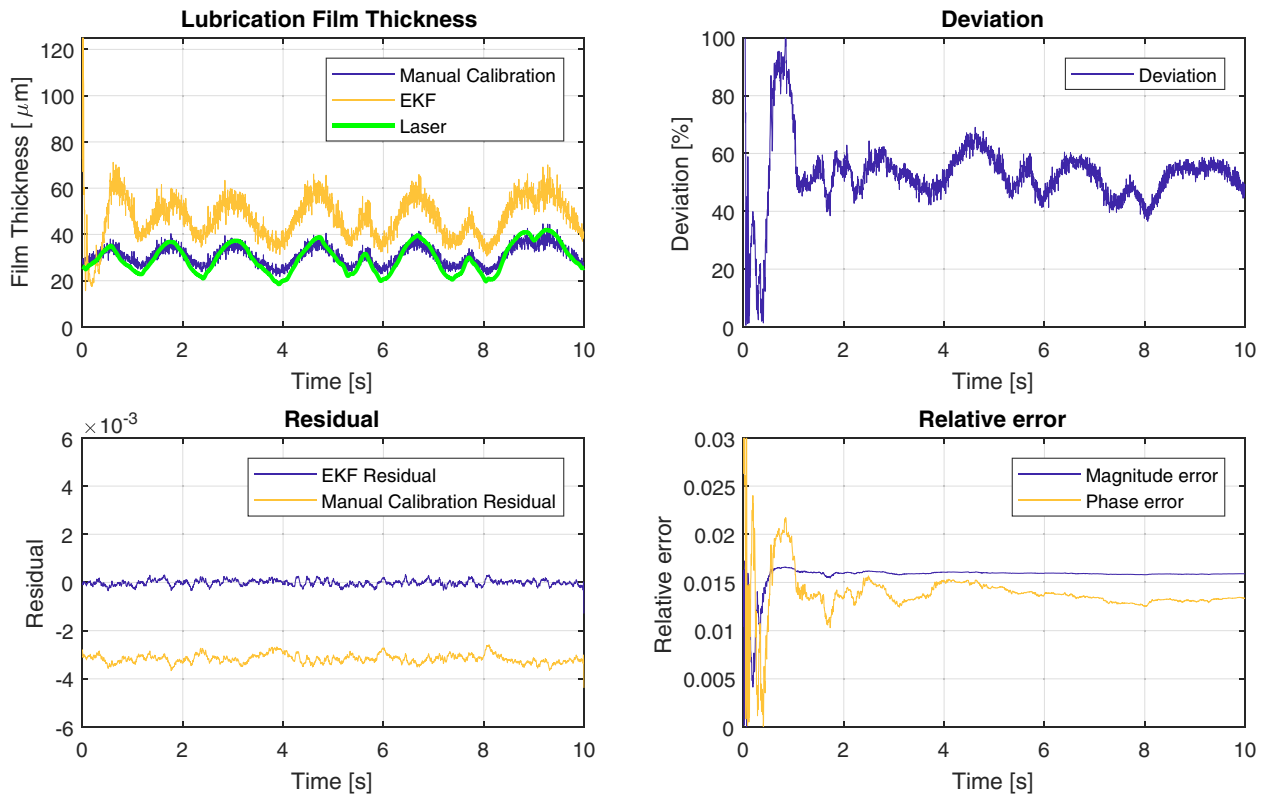


Figure 3. Dynamic thin-layer thickness testing case.

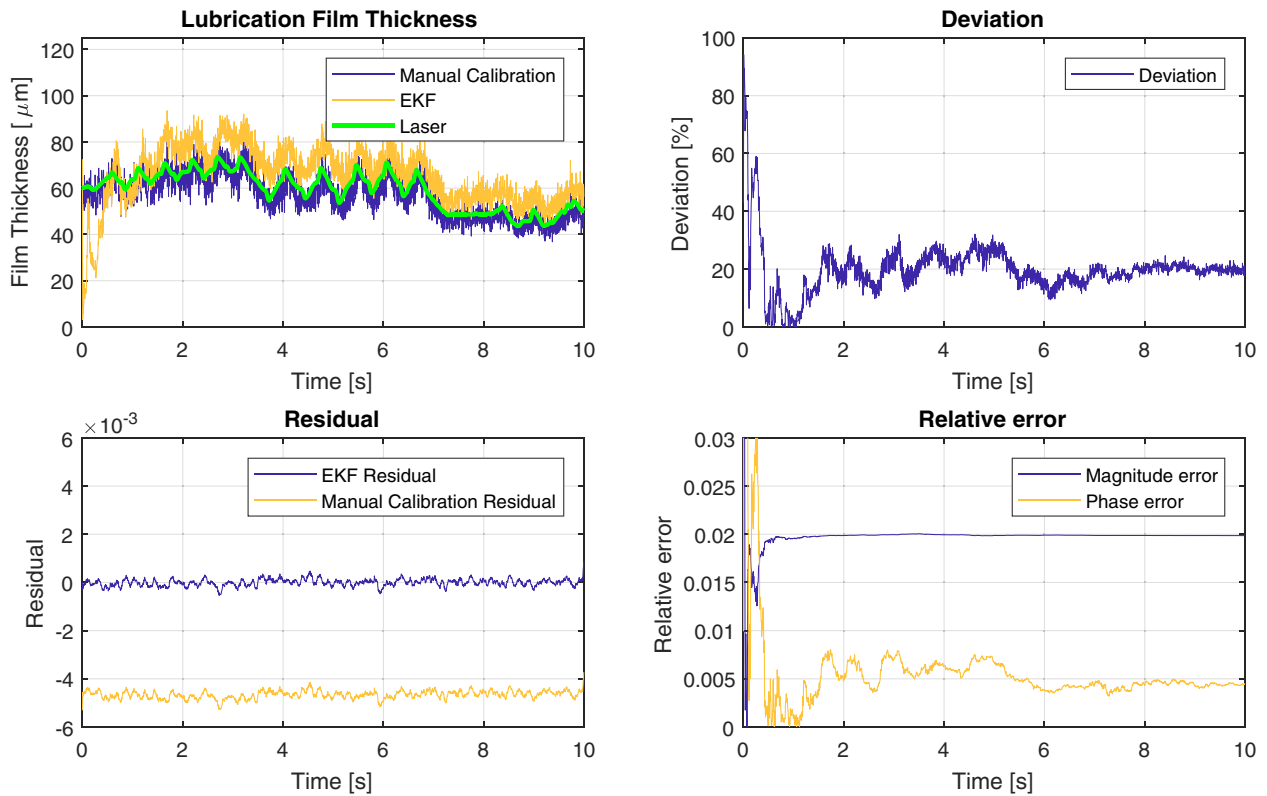


Figure 4. Dynamic thin-layer thickness testing case.

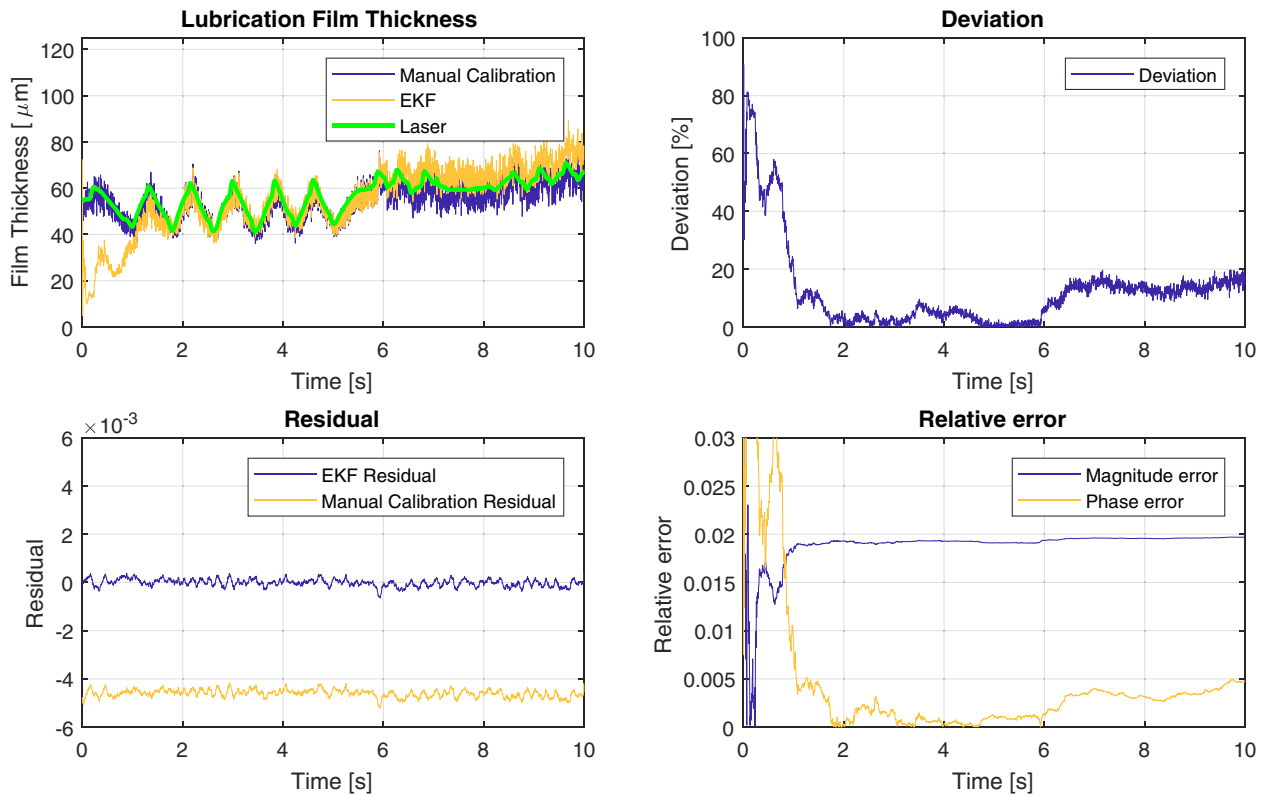


Figure 5. Dynamic thin-layer thickness testing case.

of the phase is well correlated with the deviation. It is seen that when the adaptive scheme performs well in terms of estimating the phase of the incident wave spectrum, the manually calibrated and adaptive scheme provides the same thickness results, regardless of the error in the magnitude. In order to further analyze this aspect a sensitivity analysis is performed.

### 7. Sensitivity analysis

To obtain further insights on the influence of relative error in magnitude and phase on the thickness measurements a sensitivity analysis is performed. This analysis is conducted by calculating how the change in the reflection coefficient spectrum phase shift, given as

$$\theta = \angle \mathcal{F} \{R_a(t)\} - \angle \mathcal{F} \{T_a(t)\} \quad (35)$$

affects the layer phase lag  $\angle J(\omega)$  relative to how the change in the reflection coefficient spectrum magnitude, given as

$$A = \frac{|\mathcal{F} \{R_a(t)\}|}{|\mathcal{F} \{T_a(t)\}|} \quad (36)$$

affects the layer phase lag. The layer phase-lag sensitivity is thereby expressed as

$$S = \log \left( \frac{\frac{\partial}{\partial \theta} \angle J(\omega)}{\frac{\partial}{\partial A} \angle J(\omega)} \right). \quad (37)$$

In figure 6 the layer phase-lag sensitivity is shown. Note that it is plotted as function of the layer thickness by using the constraint constituted by equation (19) and the corresponding

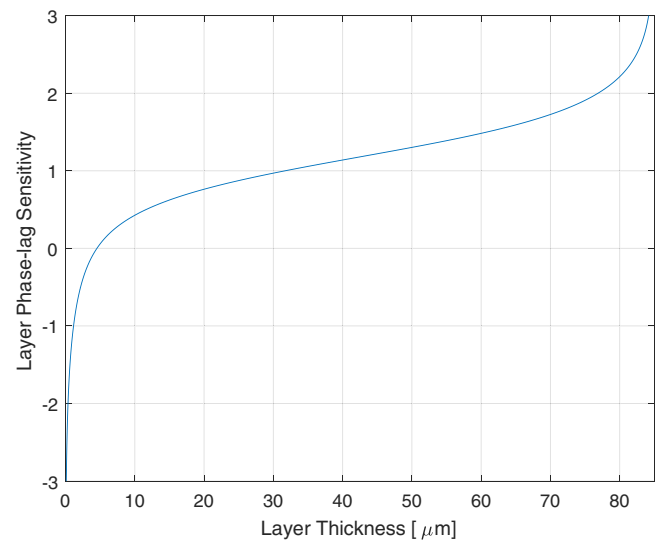


Figure 6. Layer phase-lag sensitivity as function of thin-layer thickness for a steel-oil-steel interface.

layer spectrum in equation (14). The layer phase-lag sensitivity reveals that in the ranges of layer thickness used in the test cases the phase information dominates the phase lag and thereby the thickness measurements. However, in a very thin layer  $< 1 \mu\text{m}$  the magnitude becomes dominant.

### 8. Robustness analysis

To further investigate the robustness of the adaptive ultrasound reflectometry scheme a disturbance test is performed.



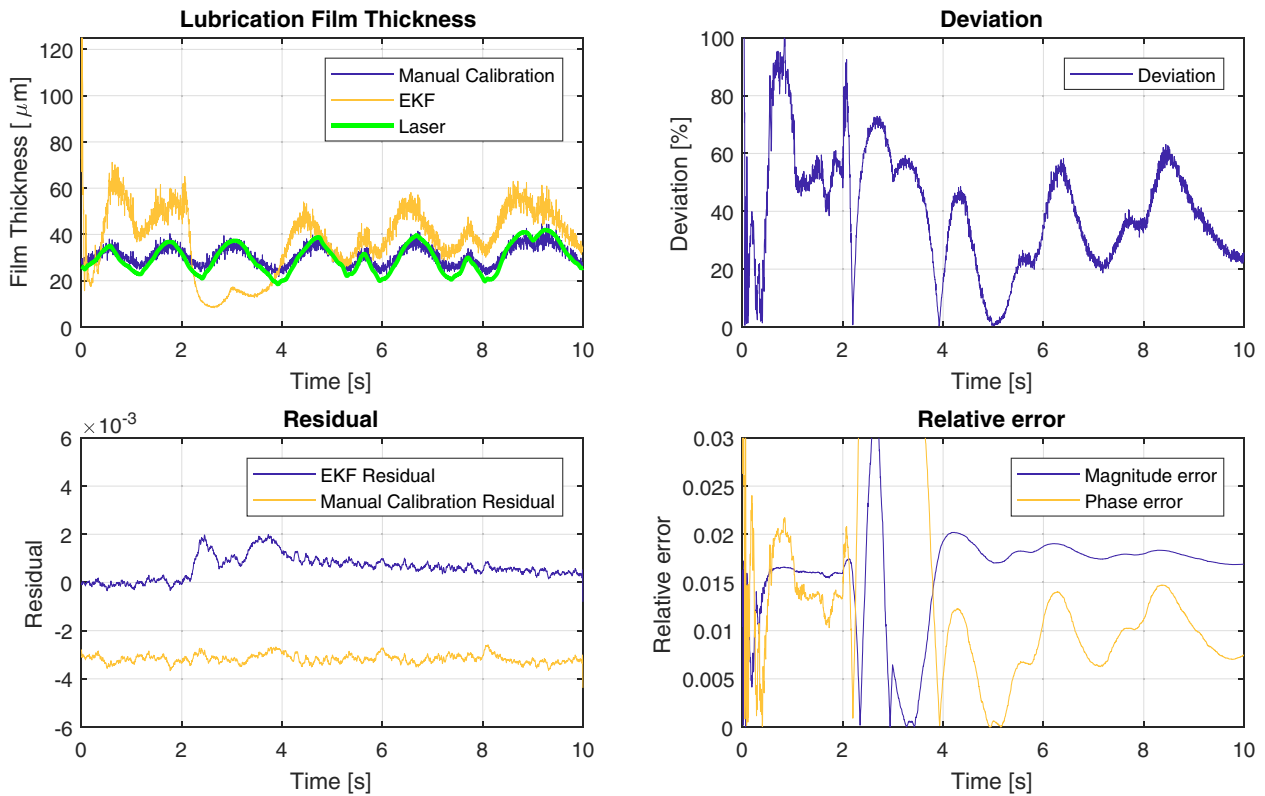


Figure 7. Dynamic thin-layer thickness testing case with a disturbance applied between 2 s and 3 s.

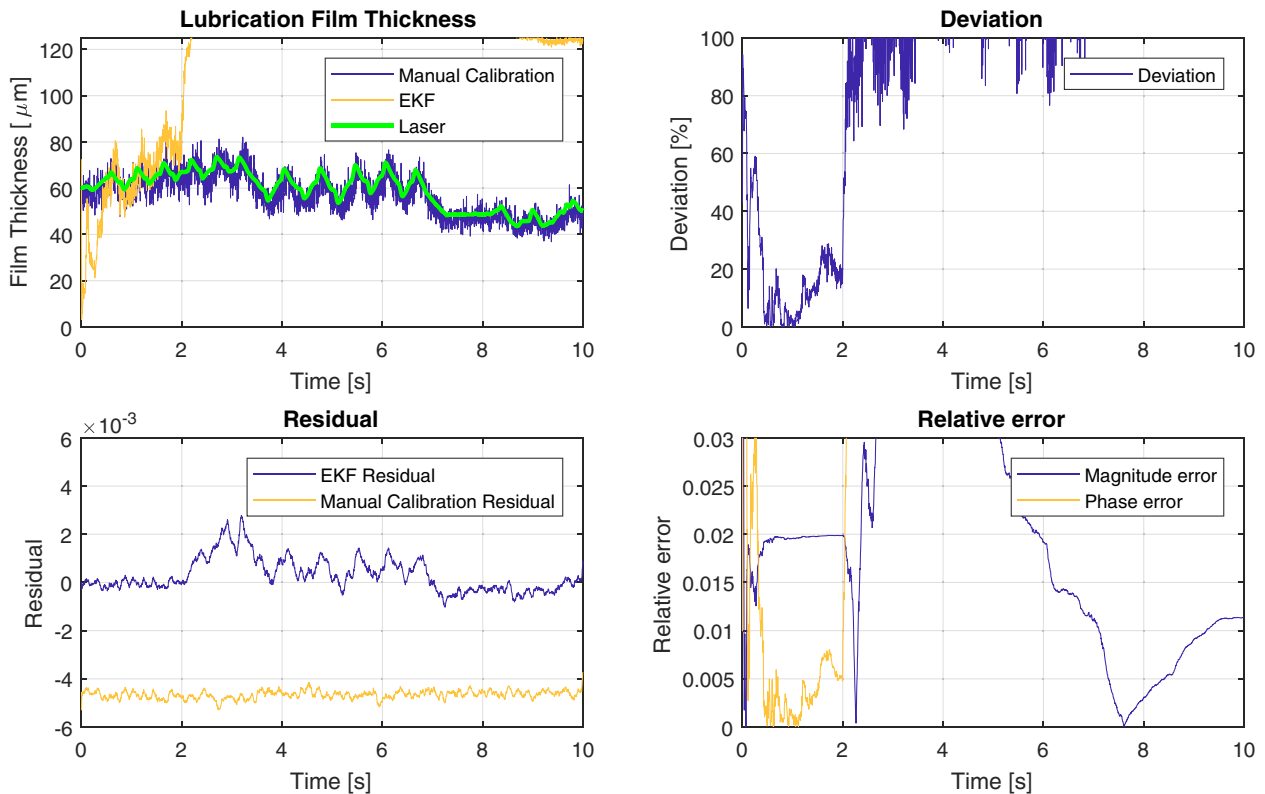
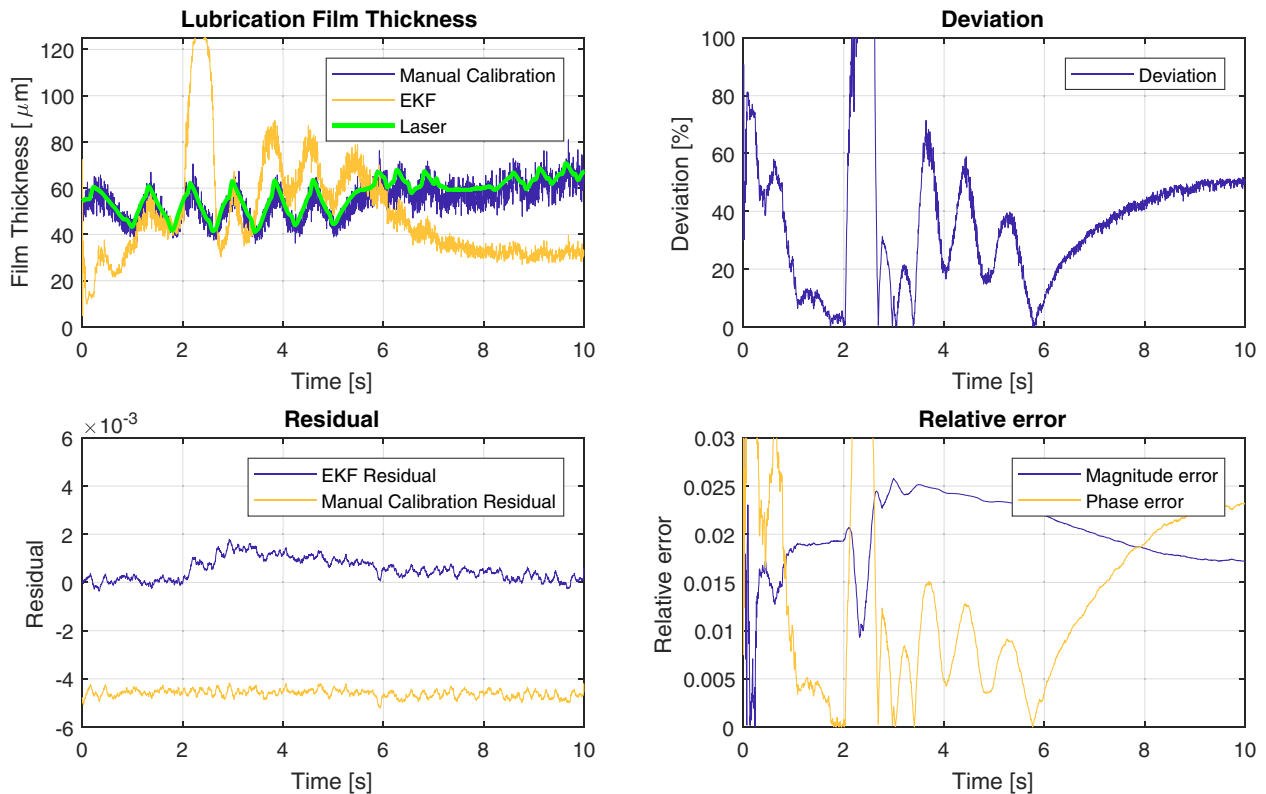


Figure 8. Dynamic thin-layer thickness testing case with a disturbance applied between 2 s and 3 s.

The test case is similar to the test in figures 3–5; however in order to emulate a temporary external disturbance the magnitude of the measured reflection  $\mathcal{F}\{R_a(t)\}$  is reduced by 2% after 2 s and restored to 100% at 3 s. This could potentially

occur if changes to the bonding of the transducer or oil contamination entailed a decrease in the energy transmitted by the transducer. The disturbance test results are shown in figures 7–9. The analysis reveal significant problems with



**Figure 9.** Dynamic thin-layer thickness testing case with a disturbance applied between 2 s and 3 s.

the robustness of the adaptive scheme. The temporary disturbance produces above 100% deviation in the test shown in figure 8, and the adaptive scheme does not seem to be able to recover. However, in the test shown in figure 9 the adaptive scheme actually recovers to decent accuracy, but after 4 s the deviation increases yet again. In all tests it is clearly seen that the relative phase error dominates the accuracy of the thickness measurements.

## 9. Conclusion

An adaptive ultrasound reflectometry method for lubrication film thickness measurements based on the layer phase-lag method and an extended Kalman filter is proposed, and experimental tests reveal the ability to provide the same accuracy in the measurement of the layer thickness variations as with the conventional manual calibration techniques. However, the tests also reveal significant problems regarding robustness and reliability of the method. Furthermore, it is shown, both in experimental testing and by a theoretical layer phase-lag sensitivity analysis, that the estimation of the incident wave phase is of high importance in the range of layer thickness present in the tests. The theoretical analysis further shows that for very thin layers below 1  $\mu\text{m}$  the estimation of the magnitude dominates the measurement accuracy.

The ultrasound methods for measurement of lubrication film thickness is a proven technology through studies on a range of applications, such as journal bearings, liner-piston skirts and internal combustion engine piston rings, and the further improvement of adaptive algorithms for auto-calibration

is an opportunity to expand the area of application for this technology. It is clear from the analysis in this work that the improvements of adaptive schemes should be directed towards phase- or magnitude-tracking performance, depending on the working range of the layer thickness, such that sufficient robustness and reliability of the algorithms can be assured.

## Acknowledgments

This work is funded by the Innovation Fund Denmark via the HyDrive-project (case No. 1305-00038B). The authors are grateful for the funding.

## ORCID iDs

P Johansen  <https://orcid.org/0000-0001-8010-283X>

## References

- [1] Johansen P, Roemer D B, Andersen T O and Pedersen H C 2015 On the influence of piston and cylinder density in tribodynamics of a radial piston digital fluid power displacement motor *ASME/BATH Symp. on Fluid Power and Motion Control*
- [2] Johansen P, Bender N C, Hansen A H and Schmidt L 2017 Investigation of squeeze film damping and associated loads *ASME/BATH Symp. on Fluid Power and Motion Control* (ASME) p V001T01A050
- [3] Johansen P, Roemer D B, Andersen T O and Pedersen H C 2014 Asymptotic approximation of laminar lubrication

- thermal field at low reduced Peclet and Brinkman number  
*J. Tribol.* **136** 041706
- [4] Geng T, Meng Q, Chen Z and Wang P 2011 Ultrasonic monitoring of lubricating conditions of hydrodynamic bearing *J. Phys.: Conf. Ser.* **305** 012065
- [5] Dwyer-Joyce R S, Green D and Balakrishnan S 2006 The measurement of liner-piston skirt oil film thickness by an ultrasonic means *Technical Paper* 2006-01-0648 SAE International (<https://doi.org/10.4271/2006-01-0648>)
- [6] Mills R, Vail J R and Dwyer-Joyce R 2015 Ultrasound for the non-invasive measurement of internal combustion engine piston ring oil films *Proc. Inst. Mech. Eng. J* **229** 207–15
- [7] Pialucha T and Cawley P 1994 The detection of thin embedded layers using normal incidence ultrasound *Ultrasonics* **32** 431–40
- [8] Zhang J, Drinkwater B W and Dwyer-Joyce R S 2005 Calibration of the ultrasonic lubricant-film thickness measurement technique *Meas. Sci. Technol.* **16** 1784–91
- [9] Dwyer-Joyce R S, Drinkwater B W and Donohoe C J 2003 The measurement of lubricant-film thickness using ultrasound *Proc. R. Soc. A* **2032** 957–76
- [10] Praher B and Steinbichler G 2017 Ultrasound-based measurement of liquid-layer thickness: a novel time-domain approach *Mech. Syst. Signal Process.* **82** 166–77
- [11] Kaeseler R L, Johansen N W and Johansen P 2018 Layer ToF methods for ultrasonic lubrication-film thickness measurements *The 6th Int. Conf. on Control, Mechatronics and Automation* (Tokyo: ACM)
- [12] Reddyhoff T, Dwyer-Joyce R S, Zhang J and Drinkwater B W 2008 Auto-calibration of ultrasonic lubricant-film thickness measurements *Meas. Sci. Technol.* **19** 045402
- [13] Kaeseler R L and Johansen P 2018 Spectrum estimation in autocalibration of ultrasonic reflectometry methods for lubrication film thickness measurements *The 6th Int. Conf. on Control, Mechatronics and Automation* (Tokyo: ACM)